Ratiometric intracellular calcium imaging in the isolated beating rat heart using indo-1 fluorescence

Otto Eerbeek, Egbert G. Mik, Coert J. Zuurbier, Martijn van 't Loo, Cees Donkersloot and Can Ince

Journal of Applied Physiology 97:2042-2050, 2004. First published Jun 18, 2004;
doi:10.1152/japplphysiol.01125.2003

Journal of Applied Physiology publishes original papers that deal with diverse areas of research in applied physiology, especially those papers emphasizing adaptive and integrative mechanisms. It is published 12 times a year (monthly) by the American Physiological Society, 9650 Rockville Pike, Bethesda MD 20814-3991. ISSN: 8750-7587, ESSN: 1522-1601. Visit our website at http://www.the-aps.org/.

J Appl Physiol 97: 2042–2050, 2004.
First published June 18, 2004; doi:10.1152/japplphysiol.01125.2003.

Ratiometric intracellular calcium imaging in the isolated beating rat heart using indo-1 fluorescence

Otto Eerbeek,[1] Egbert G. Mik,[1] Coert J. Zuurbier,[2] Martijn van 't Loo,[1] Cees Donkersloot,[2] and Can Ince[1]

Departments of [1]Physiology and [2]Anesthesiology, Academic Medical Center, University of Amsterdam, 1105 AZ Amsterdam, The Netherlands

Submitted 16 October 2003; accepted in final form 17 June 2004

Eerbeek, Otto, Egbert G. Mik, Coert J. Zuurbier, Martijn van 't Loo, Cees Donkersloot, and Can Ince. Ratiometric intracellular calcium imaging in the isolated beating rat heart using indo-1 fluorescence. *J Appl Physiol* 97: 2042–2050, 2004. First published June 18, 2004; doi:10.1152/japplphysiol.01125.2003.—Abnormalities in intracellular calcium (Ca_i^{2+}) handling have been implicated as the underlying mechanism in a large number of pathologies in the heart. Study into the relation between Ca_i^{2+} behavior and performance of the whole heart function could provide detailed information into the cellular basis of heart function. In this study we describe an optical ratio imaging setup and an analysis method for the beat-to-beat Ca_i^{2+} videofluorescence images of an indo-1 loaded, isolated Tyrode-perfused beating rat heart. The signal-to-noise ratio and the spatiotemporal resolution (with an optimum of 1 ms and 0.6 mm, respectively) made it possible to register different temporal Ca_i^{2+} transients together with left ventricle pressure changes. The Ca_i^{2+} transients showed that Ca_i^{2+} activation propagates horizontally from left to right during sinus rhythm or from the stimulus site during direct left ventricle stimulation. The indo-1 ratiometric video technique developed allows the imaging of ratio changes of Ca_i^{2+} with a high temporal (1 ms) and spatial (0.6 mm) resolution in the isolated Tyrode-perfused beating rat heart.

indo-1; ratio imaging; NADH fluorescence; calcium heterogeneity

CYTOSOLIC CALCIUM (Ca_i^{2+}) plays a critical role in cardiac function, not only in excitation-contraction coupling but also in signal transduction (second messenger), modulating a wide range of cellular functions. Changes in Ca_i^{2+} are directly related to mechanical contraction (29) and strongly affect electrophysiological properties of the heart (32) and mitochondrial function (12). Irregular Ca_i^{2+} changes can cause dangerous arrhythmias (11, 37), and disturbances in Ca_i^{2+} handling are associated with cardiac hypertrophy (18, 25), heart failure (28), and ischemia-reperfusion injury (20, 26). Noninvasive optical studies to determine Ca_i^{2+} levels are based on Ca-dependent fluorescence dyes (11a, 14). Many fluorescent tracer studies have been performed in isolated and cultured cells (36). A major drawback of this approach, however, is that isolated heart cells are not subjected to the same conditions as experienced in situ in the beating heart. Both mechanical loading and communication with neighboring cells influence the ways cardiac cells handle Ca^{2+}, which is why it is important to study the Ca_i^{2+} distribution in cardiac trabeculae (6) and in beating, intact hearts where myocardial function can be related to Ca_i^{2+}.

In whole heart studies, the techniques for the measurement of Ca_i^{2+} have been limited to localized measurements of spots on the epicardium (4) and endocardium (39), intracellular with the use of confocal laser scanning microscopy (27) or over a limited part of the left ventricular surface with the use of optical fibers guiding the illumination and fluorescence light (10). Although these techniques allowed the measurements of calcium transients, information concerning the spatial changes in Ca_i^{2+} was limited. On the basis of NADH videofluorometric studies, we have shown marked spatial heterogeneity in the energy state during ischemia (19, 13), tachycardia (2), hypertrophy (3), and endotoxemia (5). Studies where membrane potential changes on the heart surface have been imaged have also shown marked heterogeneity during arrhythmia (16, 40). This reported heterogeneity of the mitochondrial energy state as well as membrane potential changes could also be expected to give spatial heterogeneity in Ca_i^{2+}. Indeed, recently, an excellent study using diode arrays and the single-excitation, single-emission probe Rhod-2 showed that such heterogeneity in space and time in calcium transients exists (11). Use of single-excitation, single-emission dyes has the advantage of a high fluorescence yield and a less complicated optical setup. However, use of dual-wavelength dyes, such as fura-2 and indo-1, which exhibit a Ca^{2+}-dependent shift in their excitation or emission wavelength, respectively, have the advantage that they cancel out several factors influencing the emission intensity of the dyes and therefore reduce potential errors in the Ca^{2+} measurements. Such factors include fluctuation of the illumination intensity, changing dye concentration, variations in detector sensitivity, and changing optical tissue properties (17), the latter occurring during the contraction of the heart. The advantages of dual-wavelength dyes make them particularly suitable as fluorescent calcium indicator dyes for application to whole tissues such as the beating heart.

In the present study, we describe a new videofluorometric system for the measurement of Ca_i^{2+} changes in images of the surface of isolated, Tyrode-perfused, hearts using a ratiometric dye. The calcium indicator indo-1 is used as an indicator dye to image the spread of relative changes in Ca_i^{2+} on the surface of the heart in space and time. Use of the calcium indicator indo-1 requires a single-excitation wavelength of light and two emission wavelengths to be recorded (10). This so-called dual-wavelength ratio technique in combination with a video system allows visualization of Ca_i^{2+} changes in time and space (8). For such a system to work in a moving image, it is a prerequisite

Address for reprint requests and other correspondence: O. Eerbeek, Dept. of Physiology, Academic Medical Center, Univ. of Amsterdam, Meibergdreef 15, 1105 AZ Amsterdam, The Netherlands (E-mail: o.eerbeek@amc.uva.nl).

The costs of publication of this article were defrayed in part by the payment of page charges. The article must therefore be hereby marked "*advertisement*" in accordance with 18 U.S.C. Section 1734 solely to indicate this fact.

that the two images coincide exactly in space, and preferably in time, when the ratio of the images is calculated. Conventionally, in cell imaging systems, this problem has been resolved by using very fast rotating filter wheels or by using a trifurcated optic fiber bundle (10). However, these options are not applicable for the imaging of a whole beating heart via dual-wavelength dyes. In this study, an optical solution was chosen whereby a multiviewer (a combination of filters and dichroic mirrors) was used for splitting the emission light into two wavelengths and projecting the two images of the heart simultaneously on a large charge-coupled device (CCD) chip (1,317 × 1,035 pixels) of a quartz-coupled intensified slow-scan digital CCD camera. The indo-1 fluorescence ratio R (ratio of 405 nm to 485 nm) was used to express the relative Ca_i^{2+} changes during different conditions. A method for tracing patterns of Ca_i^{2+} transients and mapping the spatial and temporal heterogeneities of Ca_i^{2+} is described. This novel Ca_i^{2+} imaging technique was evaluated during electrical stimulation at various locations and during tissue injury of the Langendorff-perfused rat heart.

MATERIALS AND METHODS

Heart preparation. All procedures followed were in accordance with the Animal Ethical Commission of the University of Amsterdam. Male Wistar rats (300–350 g) were anesthetized with pentobarbital sodium (60 mg/kg iv) and heparinized (250 IU iv). Tracheotomy was performed, and ventilation was initiated. After sternotomy, the heart was taken out and rapidly submerged in ice-cold Tyrode solution. Hearts were cannulated via the aorta and perfused according to Langendorff at 37°C. The perfusion pressure was fixed at 80 mmHg, and flow was measured with an in-line flow probe (Transonic). A drain was inserted through the apex of the left ventricle to remove any Thebesian flow. The pulmonary artery was cannulated. Left ventricular developed pressure was measured with an intraventricular fluid filled balloon. The balloon was filled with fluid to obtain a diastolic pressure of 8 mmHg. Hearts were paced at 5 Hz unless otherwise stated.

Perfusion solutions. All perfusion solutions were filtered (Millipore, 0.45 μm) before use and saturated with 95% O_2-5% CO_2, resulting in a final perfusate pH of 7.4. The Tyrode solution consisted of 128.3 mM NaCl, 4.7 mM KCl, 1 mM $MgCl_2$, 0.4 mM NaH_2PO_4, 0.5 mM Na pyruvate, 20.2 mM $NaHCO_3$, 11 mM glucose, and 1.4 mM $CaCl_2$. Adequate loading of the dye was achieved by recirculating 100 ml Tyrode solution containing 5 μmol/l indo-1 AM [initially dissolved in 1 ml of dimethyl sulfoxide containing 6% wt/vol pluronic (Molecular Probes)], 5% fetal calf serum (HyClone Laboratories), and 0.1 mmol/l probenecid for 35 min at 30°C. Probenecid (Sigma), which was present in all perfusion solutions, is an anion transport blocker and has been shown to prevent loss of tetracarboxylate fluorescent indicators (1). Residual indo-1 AM was washed out by perfusing with Tyrode solution without indo-1 and 5% fetal calf serum for 30 min at 37°C. In three indo-1-loaded hearts, the contribution of endothelial fluorescence was evaluated by administration of bradykinin (10 μmol/l) (Sigma) in the Tyrode solution (10).

Ca_i^{2+} imaging. The fluorescent image of the heart was separated into two images, one at wavelength 405 nm and the other at 485 nm, by a two-wavelength multiviewer (Princeton Instruments) (Fig. 1*B*). Both images were displayed simultaneously on an image-intensifier tube (Princeton Instruments PP0304N, 25-mm S20 red enhanced photocathode) by a 105-mm macro lens (Nikon). Via a relay lens (PI 1:1, F = 1.7) the intensified image was projected on a cooled CCD camera (Princeton Instrument Pentamax 1317 K, 1,317 × 1,035 pixels). The image intensifier was connected to a gating pulse generator and power supply unit (PG200, PI), which gated the image intensifier so that it functioned as an extremely fast shutter device.

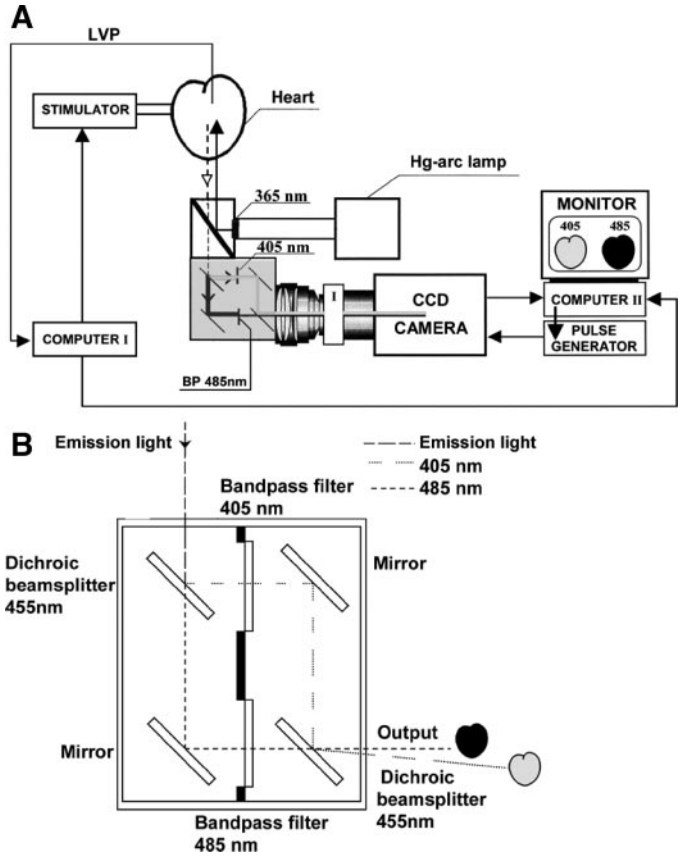

Fig. 1. *A*: schematic diagram of the dual-wavelength videofluorometric measurement system. The 365-nm excitation light, which is provided by a 100-W Mercury (Hg) arc lamp, is selected by a 365-nm filter (UG-1 filter). DCLP 390 is a dichroic mirror in the beam splitter, which is translucent for wavelengths higher than 385 nm. *B*: the dichroic mirrors DCLP 455 are translucent for wavelengths higher than 455 nm. Both light paths use filters 405 ± 10 nm and 485 ± 20 nm, respectively. Both images are projected simultaneously on the cathode (I) of a second-generation image intensifier tube by a macro lens (Nikon). Via a lens-coupled system, the intensified image is projected on the charge-coupled device (CCD) of a cooled video camera. BP, band-pass filter; LVP, left ventricular pressure.

Two computers were used to acquire the data and to control the experiment. *Computer I* was configured as a data acquisition system for the following parameters: perfusion pressure, flow, left ventricular pressure, and temperature. This computer also provided the main trigger pulse, generated by the data acquisition board in this PC (National Instruments Lab PC+), triggering both the heart stimulator and the delay generator in *computer II*. *Computer II* was used for image acquisition and control of the camera system. The main trigger pulse triggered the timer-counter circuit on the acquisition board in *computer II* (NI AT-MIO-16E-10) to generate a delayed trigger pulse to the gating pulse generator and image acquisition system. The delay had a preset increment (typically 1 or 10 ms) for subsequent trigger pulses, resulting in a sequence of images covering a whole heart cycle at evenly spaced points in time. The hardware timer available on the data acquisition board was used to prevent the time jitter usually present in software-based timing. Both computers were programmed with Labview graphical programming software (version 5.1, National Instruments). Image acquisition was performed on *computer II* by use of WinView software (Princeton Instruments) (Fig. 1).

Two different series of experiments were performed (*series A* and *series B*). In *series A* with *setup A*, an exposure time (on chip-

integration time) of 10 ms with an increment in trigger delay of 10 ms was used. These recording conditions are ultimately appropriate for recording the temporal Ca_i^{2+} changes of the whole ventricle. In this setting, a whole heart cycle of 200 ms (pacing rate 5 Hz) was captured in 20 images (i.e., over 20 beats). In *series B*, with the *setup B*, an exposure time of 1 ms and an increment of 1 ms was used. To allow image acquisition with this higher temporal resolution without a significant decrease in signal to noise ratio, the sensitivity of the image-acquisition system had to be improved. A 4 × 4 on-chip averaging (binning) of pixels was applied to compensate for the light loss as a consequence of the shorter integration time. Although binning reduces the spatial resolution of the image-acquisition system, both the detection sensitivity and readout rate were increased in this manner. This configuration (*setup B*) allowed the recording of a whole cycle in 200 pictures (i.e., over 200 beats) each lasting 1 ms and enabled the registration of interregional different starting times of Ca_i^{2+} changes on the surface of the left ventricle (spatiotemporal heterogeneity of Ca_i^{2+} transients) during one heart cycle. In both setups, a 100 W mercury arc lamp in combination with a UG-1 filter provided an excitation wavelength of 360 nm, which was projected onto the heart by a beam splitter in front of the multiviewer, resulting in a homogeneous illumination of the heart.

Image processing. In *series A* and *B*, the autofluorescence in both recorded wavelengths (405 and 485 nm) during the whole heart cycle was recorded before indo-1 loading of the isolated heart. Autofluorescence at 485 nm corresponds to NADH fluorescence, an expression of the metabolic state of the tissue. The two-wavelength recorded autofluorescence sequences were used to correct for autofluorescence and background signal in the calculation of the indo-1 ratio, by subtracting the mean intensity before indo-1 loading from the mean intensity of the same area of interest after indo-1 loading (15). *Series A* ($n = 5$) has been analyzed with the statistics option available in the WinView software. The mean intensity of a large part of the left ventricle was measured for both the 405- and 485-nm images individually by choosing an appropriate area of interest. The same area of interest was used for both the autofluorescence images of the unloaded heart and the fluorescence images of the indo-1-loaded hearts (*setup A*).

To allow detection of heterogeneity of Ca_i^{2+} levels in the time course of the indo-1 ratio changes over the surface of the heart, *series B* had to be analyzed in more detail. To match the 405- and 485-nm images precisely, pixel by pixel, a small light spot produced by a fiber-optic light guide connected to a xenon arc lamp was recorded next to the heart during the experimental protocol. This spot was visible in both the 405-nm and 485-nm images, allowing the spot to act as a reference point for pixel-to-pixel analysis. After the coordinates of the spot in both images were defined, a program written in Labview (extended with the IMAQ package) was able to calculate the background-corrected indo-1 ratio per pixel for all recorded images during the heart cycle. To improve the signal-to-noise ratio in the final analysis of *series B*, the resulting pictures were software binned, resulting in a matrix pattern of indo-1 ratios covering the original image of the heart. The size of the binning area could be selected. For the analysis, either a 5 × 5 squared matrix (spatial resolution 1.8 mm) (Fig. 2) or a 15 × 15 squared matrix (spatial resolution 0.6 mm) was used. In both cases, the signal to noise ratio was adequate to detect temporal differences of Ca_i^{2+} ratios. The time course of the indo-1 ratio per area was filtered by a median filter before it was transferred to a spreadsheet file. This filter takes the median value of five samples, i.e., the current sample point (regarded as $t = 0$ ms) and the four surrounding sample points ($t = -2, -1, 1$, and 2 ms). Periodic signals up to 20 kHz pass this filter undistorted; this is well above the required frequency of 4 kHz (using a sampling frequency of 1 kHz).

In this final format, the time course of the indo-1 ratios of the individual image areas could be visualized in an almost online fashion (*setup B*).

Experimental protocol. After a 15-min equilibration period, hemodynamic parameters and background fluorescence were measured in the experimental setup. Thereafter, the hearts were loaded with indo-1 AM in the same setup (see *Perfusion solutions*). After loading, the hearts were divided in two groups, *group A* and *group B*, corresponding with *setups A* and *B*, respectively.

In *group A* ($n = 5$), the hearts were stimulated through two leads attached to the right ventricle, and *setup A* was used for measurement and analysis of the corrected indo-1 ratio signal in combination with the left ventricle pressure. Visual inspection of the autofluorescence

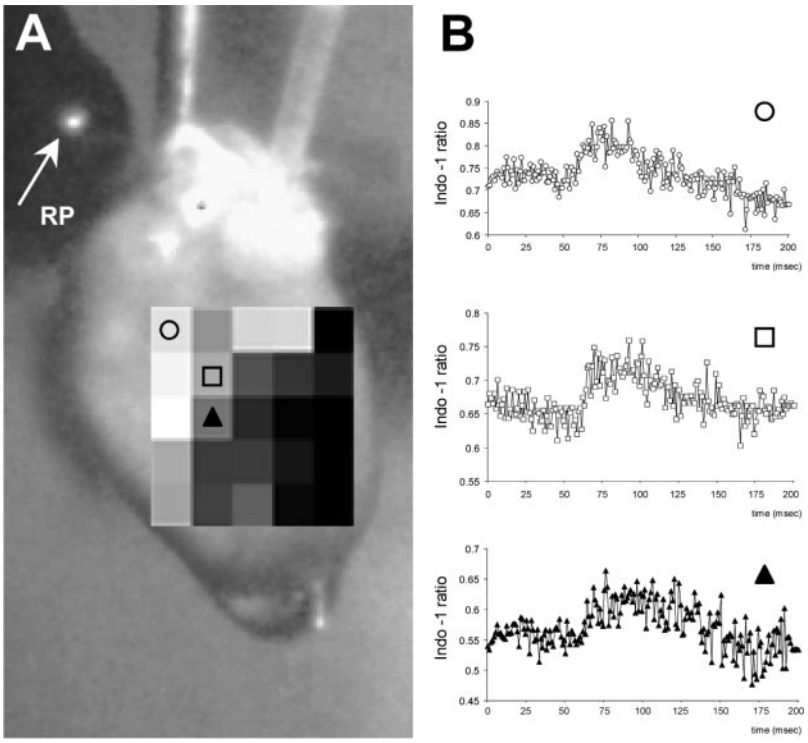

Fig. 2. *A*: a heart image is shown on which the 5 × 5 matrix pattern (spatial resolution 1.8 mm) is superimposed to illustrate how the spatial dependency of the cytosolic calcium (Ca_i^{2+}) was analyzed. The whole matrix, including the uppermost left part, is covering the left ventricle of the heart. Symbols are the same as in Fig. 6 (symbols are associated with that heart position). RP, reference point for the image processing. *B*: the 3 traces show the indo-1 ratio signals of the 3 selected areas during a whole heart cycle before filtering.

and indo-1 fluorescence was used to confirm uniform loading. Additionally, the contribution of the endothelial fluorescence to total fluorescence was evaluated in three hearts of this group by switching to a Tyrode solution containing 10 μmol/l bradykinin for a period of 15 min.

In *group B* ($n = 3$), the left ventricle was either stimulated naturally by right atrium stimulation, allowing propagation through the bundle of His, or directly by placing the concentric bipolar electrode on the left ventricle. Measurements and analysis were done using *setup B*. The potential influence of motion of the heart was evaluated by pharmacological inhibition of contraction by 20 mM 2,3-butanedione monoxime [= diacetyl monoxime (DAM)] (23, 34).

RESULTS

To determine whether autofluorescence changes occur during the heart cycle and during the measurements, two experiments were performed using detection at 450 nm with the use of an uranyl as external reference. In these experiments, we measured the NADH signal (autofluorescence) at the beginning of the experiment and 60 min later. During this period the loading procedure with calf serum was performed without the addition of indo-1. The NADH signal was measured during the first 100 ms of the heart cycle in 1-ms steps. The results of both experiments are shown in Fig. 3. At both time points (start of experiment and 60 min later), no transient changes in the NADH fluorescence emission were detectable during the first 100 ms of the heart cycle. The overall autofluorescence changed by ~5–10% over the entire experiment (one experiment showed a decrease of 5%, the other and increase of 10%). As reported below, indo-1 loading leads to a 400–600% increase in signal intensity at 485 nm. Compared with the indo-1 signal, the change in NADH signal during the experiment was negligible. We therefore believe that the background correction of the ratio measurements with the NADH signal measured at the start of the experiment is appropriate.

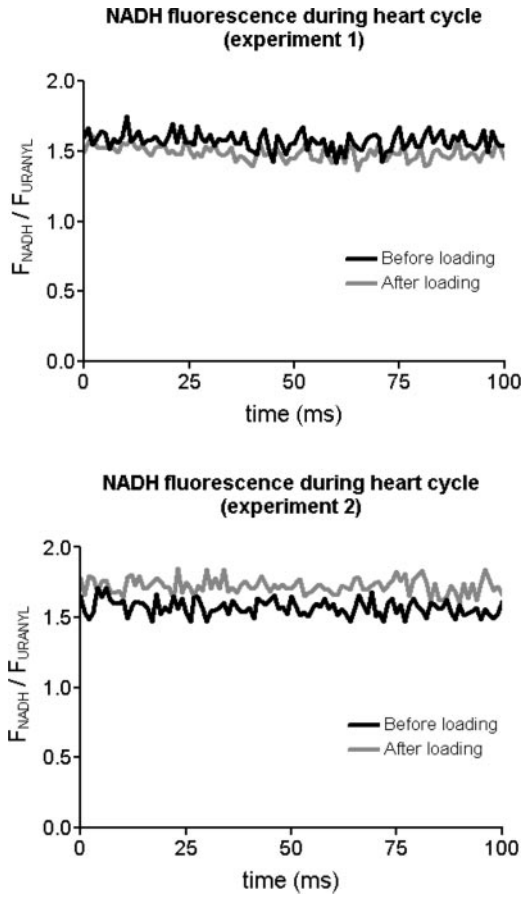

Fig. 3. NADH autofluorescence (F_{NADH}/F_{uranyl}) measured at 450 nm, during the first 100 ms of the heart cycle, before and after a mimicked loading procedure.

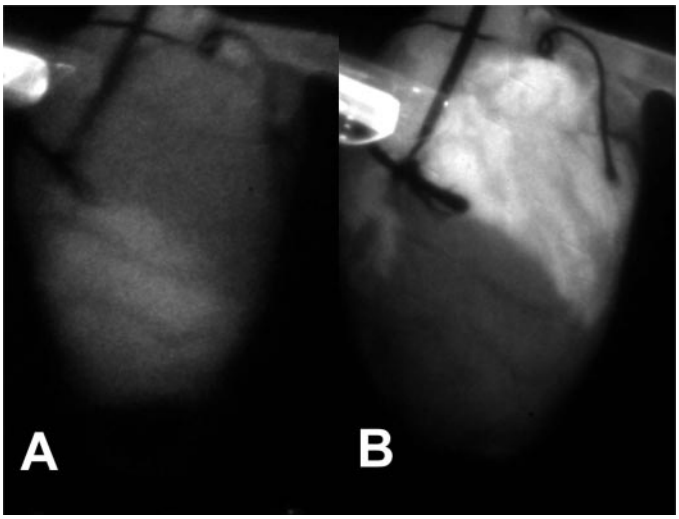

Fig. 4. Two images are shown at 485 nm. *A*: NADH image (485 nm). *B*: the same heart after loading with indo-1 at the same wavelength.

During the loading procedure, a change in pressure development was present (data not shown). This change concerned both an increase in diastolic pressure and a decrease in systolic pressure and therefore a decrease in overall developed pressure. However, after the washout period, these changes reversed to the situation before loading with indo-1 (peak tension reduction 0–20%). We therefore assume that the observed change in pressure development was due primarily to an effect of the low temperature during the loading procedure (temperature = 30°C) and not to intracellular calcium buffering by the dye.

The loading procedure increased total fluorescence of the heart by a factor of 4–6 compared with the autofluorescence measured before loading. Verification of homogeneous loading of the heart by indo-1 is essential for performing reliable Ca_i^{2+} measurements over the surface of the heart. This proposed new technique of imaging allowed evaluation of the success of the loading procedure and detection of damaged areas on the surface of the heart. To illustrate how the presented imaging setup allows visual identification of spatial abnormalities, we present two examples. The first example shows inhomogeneous loading of the heart (Fig. 4). In Fig. 4*A*, a high level of autofluorescence, indicative of ischemia probably due to obstructed regional circulation, is seen in the lower part of the heart. After loading with indo-1, the upper part of this heart increases in fluorescence intensity, whereas the lower part remains unloaded (Fig. 4*B*). In the second example, the loading procedure was successful, but a slight injury was evoked by pinching a small area of the left ventricle surface with a forceps, after indo-1 loading. Figure 5 illustrates this small area as a black image at the 485-nm wavelength and a complementary white area at the 405-nm wavelength, indicative of a high local Ca_i^{2+} concentration.

A total of eight successful experiments was performed. In all cases a temporary distinct increase in indo-1 ratio fluorescence increase (6–16%) related to the Ca_i^{2+} transient during cardiac contraction was observed. Bradykinin administration did not change the diastolic and systolic ratio levels, indicating the limited endothelial contribution to the signal (10, 24).

Figure 6 illustrates how the time course of the Ca_i^{2+} transient of a large part of the left ventricle related to the time course of the simultaneously recorded left ventricular pressure (Fig. 6). A sharp rise in the indo-1 ratio was observed with the peak preceding the pressure peak (mean delay time of 46 ms), followed by a slow fall in indo-1 ratio. To illustrate that the indo-1 ratio change is caused by the Ca_i^{2+} transients in the heart cells, the hearts were paced at various frequencies, and in all cases the number of indo-1 ratio transients per time unit corresponded with the number of stimulation pulses in that time period.

Figure 7*A* (0–100 ms) shows the time course of the indo-1 ratio at three locations during the heart cycle. The Ca_i^{2+} transient of the lateral square (○) started before the two other squares in the longitudinal axis (showing the same timing, □ and ▲). Figure 7*B* shows the time course of the indo-1 ratio during the first 100 ms for the same locations, but now during inhibition of contraction with DAM. Application of 20 mM DAM completely blocked pressure development, and therefore these results indicate that the observed calcium transients are not due to motion artifacts.

Figure 7, *C* and *D*, shows the effect of direct left ventricle stimulation vs. right atrium stimulation on the time course of the indo-1 ratio for the similar locations on the heart. These panels demonstrate that the developed imaging technique clearly shows the different regional time courses of the calcium transient anticipated by the different location of excitation.

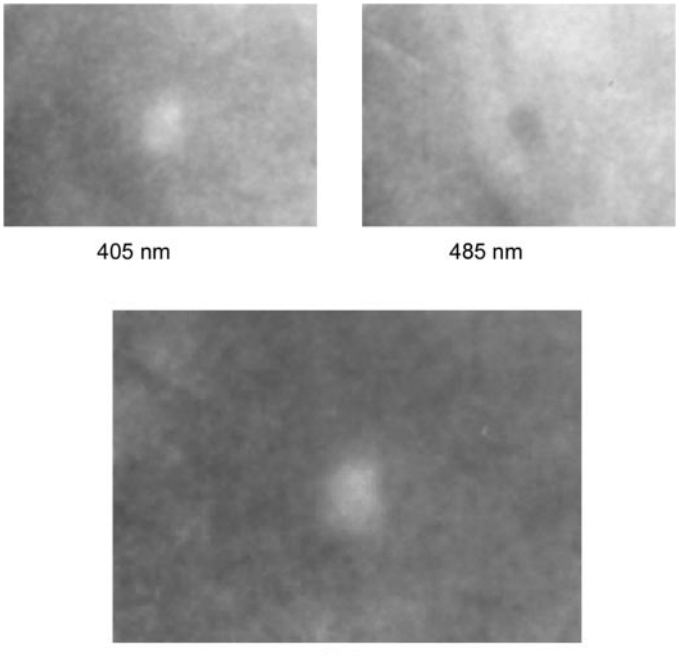

Fig. 5. Image at both wavelengths (405 and 485 nm) and the ratio image after a small lesion (pinching the tissue) on the epicardium of an indo-1-loaded heart.

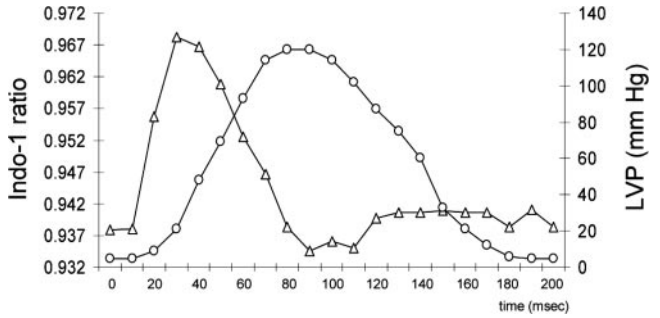

Fig. 6. Time course of the indo-1 ratio (△) and the left ventricular pressure (○) during a whole heart cycle of 200 ms (pacing frequency 300/min). The indo-1 ratio is corrected for the autofluorescence.

Figure 8 demonstrates clearly in two different hearts that, when using a higher spatial resolution than used in Fig. 7 (squared matrix 15 × 15, spatial resolution 0.6 mm), different regional time courses of the calcium gradient are still detectable.

From Figs. 7*A* and 8 it appears that the delay in calcium transient is especially apparent in the horizontal direction, whereas the activation in the vertical direction is nearly simultaneous. To study this phenomenon in more detail, a slightly adapted method of analysis was performed in two hearts. In this analysis, the averaging of seven areas of 0.6 × 0.6 mm, resulting in a detection area of 0.6 × 4.2 mm in both vertical and horizontal directions, was used to analyze a small portion of the left ventricle in detail (Fig. 9*A*). This increased a signal-to-noise ratio by the square root of 7, while maintaining the spatial resolution of 0.6 mm in the direction of interest. Figure 9*B* shows the results of this analysis for one heart. It is clear that binning in the vertical direction and performing the analysis in the horizontal direction results in a time delay in the calcium transients from *panels 1* to *7*. In contrast, horizontal binning and subsequent vertical analysis reveals no delay in calcium transients at all. The results in the second heart were similar, i.e., a delay in calcium transient of 10 ms over 4.2 mm in the horizontal direction and no delay in the vertical direction.

DISCUSSION

The aim of this investigation was to develop a ratiometric, videofluorometric system to measure the temporal and spatial distribution in Ca_i^{2+} during the cardiac cycle on the surface of intact beating Tyrode-perfused Langendorff rat hearts. This study made use of the dye indo-1, which exhibits a Ca^{2+}-dependent shift in its emission wavelength. Imaging both emission wavelengths simultaneously and analyzing the ratio image has the advantage that potential errors in Ca^{2+} measurements are reduced. For example, fluctuations in illumination intensity, changing dye concentration, variations in detector sensitivity, and changing optical tissue properties are confounding factors that are cancelled out by the ratio imaging method (17). Furthermore, incomplete hydrolysis of the 2-AM esters does not invalidate the outcome of the ratio measurements within one heart (35). This study describes and validates such a system, based on a commercially available optical multiviewer and an image-intensified slow-scan camera. The use of an optical multiviewer that projects two images of the

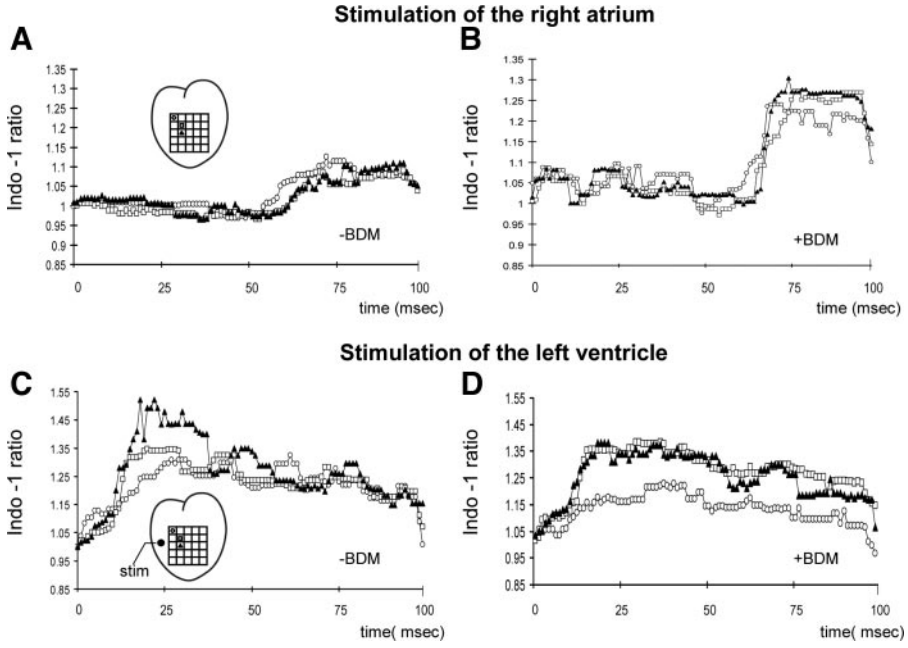

Fig. 7. Time course of the indo-1 ratio of the 3 squares ○, □, and ▲ (positions shown in Fig. 2*A*) produced with a 5 × 5 matrix (spatial resolution 1.8 mm) during a heart cycle of 200 ms (pacing frequency 300/min). *A* and *B*, with stimulation of the right atrium, and *C* and *D*, with direct stimulation of the left ventricle, show the time course of the indo-1 ratio. *B* and *D* after addition of 2,3-butanedione monoxime (BDM) (= diacetyl monoxime DAM). *Inset* in *A* and *C* shows the schematic heart with the position of the 3 squares in the matrix and in *C* also the position of the stimulation electrode (stim).

heart (both emission wavelengths) on one single (large) CCD has two major advantages: both wavelengths are recorded truly simultaneously, and a variation in detector sensitivity affects both wavelengths in the same manner and therefore does not affect the ratio. In the presented study, we validate the system and present temporal and spatial changes in Ca_i^{2+} in the isolated, nonrestrained beating rat heart.

By using dual-wavelength imaging, values of Ca_i^{2+} were expressed in terms of the ratio of two wavelengths (18, 32). The analysis was limited to ratio measurements, because the determination of absolute values of Ca_i^{2+} is difficult in the intact heart (7) and not truly necessary for detection of spatiotemporal heterogeneity (calcium wave). Furthermore, incomplete hydrolyzation of the indo-1 AM ester in the heart is an unpredictable factor influencing the emission at 485 nm (and thus influencing the ratio), making it virtually impossible to make a valid one-time calibration (35). However, ratio changes within one heart are representative for calcium changes, and our results demonstrate that the indo-1 AM fluorescence ratio provides a good method for semiquantitative analysis of heart tissue Ca_i^{2+} concentration changes. The time to peak of the Ca_i^{2+} transient and the time delay between the peak of the Ca_i^{2+} transient and left ventricle pressure in this study agree with values found by Meisner and Morgan (26).

One of the major technical difficulties for optical measurements in situ is the mechanical movement of the heart during contractions. Brandes et al. (9) reported that using the dual-wavelength ratiometric technique reduces the motion artifact by a factor of five. With this technique, the motion affected the indo-1 ratio by <10%. In addition, it should be noted that our system is less sensitive for motion artifact than other reported systems (e.g., photomultiplier fiber systems) because of the long working distance (14 cm compared with 1 mm with fibers). By attaching a suture needle to the surface of the heart, we were able to obtain estimates of the movement in the *xy*-plane. The maximal movement amounted to 0.47 mm, primarily in the horizontal direction. Our analysis was performed not on a pixel-to-pixel basis (although this is theoretically possible) but on binned areas of pixels. For our analysis with the 5 × 5 matrix, the spatial resolution of the system is 1.8 mm. Therefore, the maximal theoretical contribution of translations in the surface of the heart relative to our binned area of pixels is 25%.

The electrical activation order of the cardiomyocytes is expected to provide a similar time course and direction as that of the propagation of the Ca_i^{2+} wave. Indeed, the observed lateral direction and temporal differences between Ca_i^{2+} transients in this study coincide with results obtained with potential-sensitive dyes (33).

An advantage of the ratiometric CCD video imaging system is that no direct contact between the measurement device and tissue is needed, allowing unrestrained motion of the heart. In fiber-optic measurements, motion artifacts are reduced by a direct contact of the fiber with the heart and/or restriction of the heart by placing it into a chamber or by compensating algorithms (9). However, it is highly conceivable that compression on the surface of the heart, due to restriction methods designed for reducing motion artifacts, will cause interference with Ca_i^{2+} levels. Using NADH videofluorometry, we found that even the slight compression induced by a glass coverslide onto the heart surface can substantially alter the hemodynamics of microcirculatory units present on the heart surface. In addition, stretch-activated ion channels can allow rises in Ca_i^{2+} (38). Furthermore, fiber measurements cannot detect the presence of inconsistencies or small regional damages on the myocardium surface that may influence measurements (e.g., Fig. 5).

Dye distribution among the different cell types in the heart could be a potential source of error in attempts to analyze the indo-1 fluorescence values for ratio measuring. Under the assumption that bradykinin promotes the same calcium influx in endothelial cells in rat as in rabbit, our bradykinin experiments indicated that endothelial contribution to the indo-1 fluorescence can be neglected (10, 24). There are indications that indo-1 may transverse the mitochondrial membrane (10).

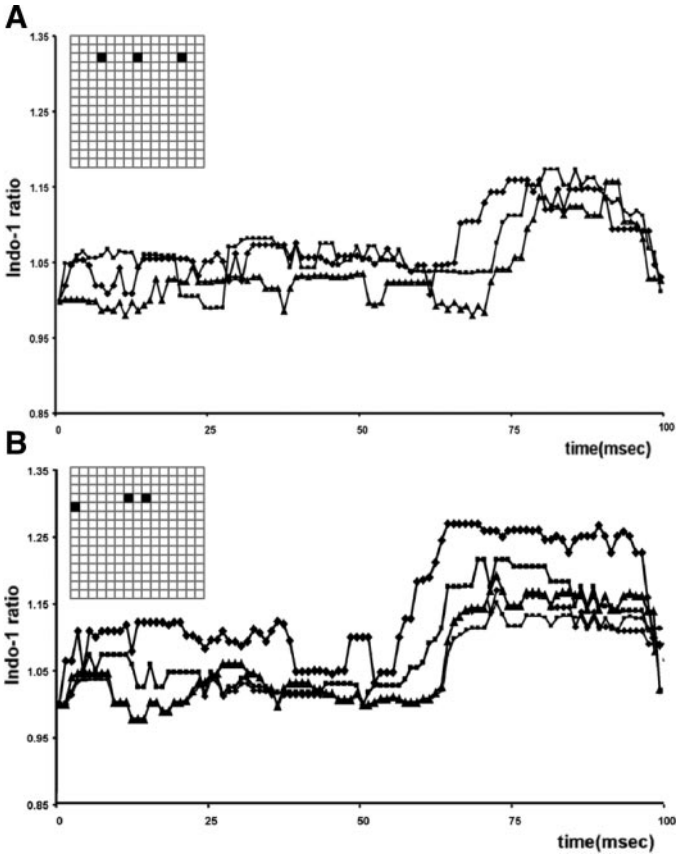

Fig. 8. *A* and *B*: time courses of the indo-1 ratio at different locations in 2 different hearts (positions shown in each matrix) produced with a 15 × 15 matrix (spatial resolution 0.6 mm) during the first 100 ms of the heart cycle (pacing frequency 300/min). In the horizontal direction a delay in calcium transients is present from left to right.

Loading conditions applied in this study (loading at 30°C) have showed in rabbit heart that fluorescence from isolated mitochondria was only 3.6% of total fluorescence (22). Loading of the dye into mitochondria of rat heart, however, should not be excluded when interpreting Ca_i^{2+} measurement using fluorescent dyes (35). During our indo-1 loading procedure, the developed force decreased to 50%. After indo-1 washout, peak tension was only 0–20% lower compared with the preloading conditions, indicating that the indo-1 Ca_i^{2+} buffering was low and the kinetic properties were fast enough to adequately assess Ca_i^{2+} transients in myocytes (10). We also showed that the NADH background fluorescence minimally affected our indo-1 transients. On the basis of these observations, we conclude that the indo-1 ratio changes are predominantly produced by cytosolic calcium changes.

Compared with other studies, and in particular those using single-excitation emission dyes, the signal-to-noise ratio of our system is relatively low. This is partly due to the relatively complex optical setup (Fig. 1) in which the loss of signal occurs and partly due to the detector that was utilized (image-intensified slow-scan camera). The optical setup, necessary for simultaneous imaging at two wavelengths, causes significant attenuation (~90%) of the detected emission light. This loss of light is due to imperfect light transmission of dichroic beam splitters, band-pass filters, and the faraway position of the focusing lens in combination with the multiviewer. The detector we used is a cooled CCD, which is inherently less sensitive than detectors like photomultiplier tubes. Image amplification at a high gain was necessary to be able to take images with integration times of 1 ms, but the use of image amplifiers comes at the expense of noise. Finally, the noise in the

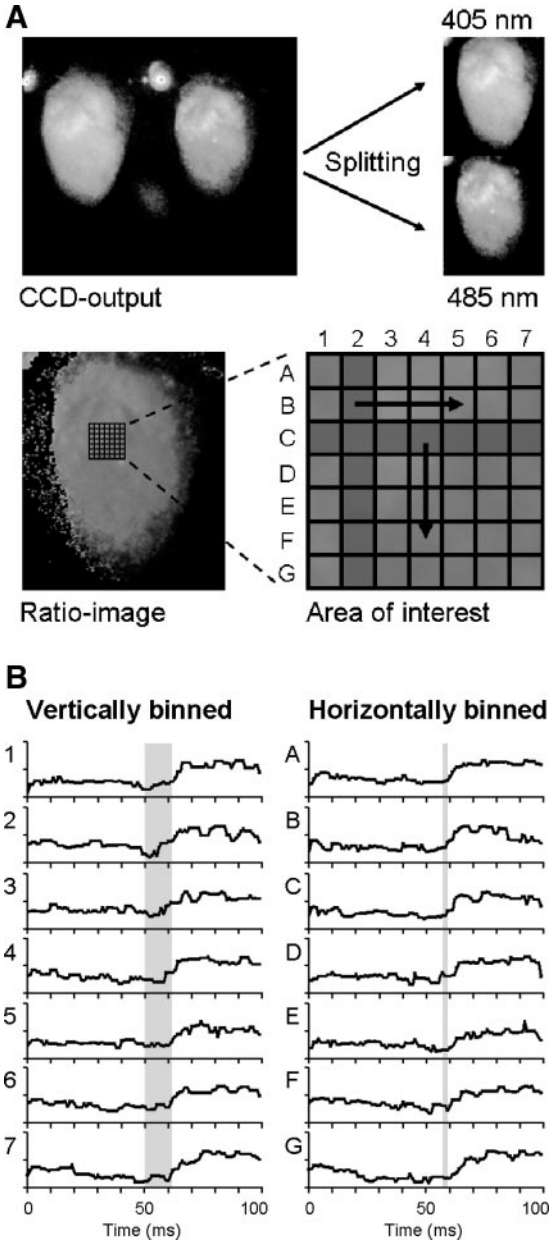

Fig. 9. *A*: steps taken from the acquired image from the CCD to a detailed analysis of calcium transients in a small portion of the left ventricle. The splitting of the CCD output into 2 images, representing the 405- and 485-nm wavelengths, is performed by using the 2 reference points (see MATERIALS AND METHODS). The contrast and brightness of the ratio image (image at 405 nm divided by the image at 485 nm) is optimized to show more clearly the region of interest. It is clear that the ratio method is effective in canceling out inhomogeneities in the fluorescence at the single wavelengths. The area of interest is 4.2 by 4.2 mm and was analyzed by dividing it in 7 parts in either the horizontal or vertical direction. *B*: results of the analysis in both the horizontal (vertically binned) and vertical (horizontally binned) direction from 1 heart. In the horizontal direction, a delay in calcium transients is present from the left (*1*) to the right (*7*). This delay is absent in the vertical direction.

resulting images is amplified by a factor of two when taking the ratio image (noisy image divided by another noisy image).

The use of single-excitation, single-emission dyes allows a less complicated optical setup. Higher fluorescence yield dyes like Rhod-2 and Fura-red (compared to indo-1) combined with simpler, but more sensitive, detectors provides an advantage in terms of signal-to-noise ratios. In contrast, ratio imaging, as developed in this study, is advantageous in terms of reduced motion artifacts, and the possibility of visual inspection of regional loading and surface artifacts. Moreover, the ratiometric imaging technique we have developed competes in spatial resolution (and has the potential for even higher spatial resolutions) with other techniques described in the literature (11, 21). For example, Choi and Salama (11), using a diode array system and the single-excitation dye rhod-2, reported calcium transients in the whole heart resembling the transients shown in Fig. 2, except that their transients were smoother and did not show the fast decay at the end of each curve. These differences are probably due to the different filtering techniques used. The curves shown in our Figs. 7–9 were filtered with a running median filter to reduce noise and clarify the time difference in start of upstroke of calcium transients. A median filter was chosen instead of an averaging filter (e.g., Bessel) because in very noisy signals the latter type spreads out noisy peaks in time, mimicking a transient. A median filter behaves better in this respect, but the drawback is the less smooth result produced. The fast decay at the end of each curve (indeed the most pronounced in Figs. 7B and 8) is an artifact introduced by the utilized filter.

The data provided in Figs. 7–9 indicate the presence of a calcium wave over the surface of the heart. The detailed analysis performed in Fig. 9 shows that this wave is more pronounced in the horizontal direction (i.e., transversal). This phenomenon can be explained by assuming different conduction velocities in longitudinal and transversal direction, as is described in the literature (31).

In conclusion, our study demonstrates that the developed indo-1 ratiometric video technique allows the imaging of ratio changes of Ca_i^{2+} with a maximal temporal resolution of 1 ms and spatial resolution of 0.6 mm. This technique is suitable for the study of the dynamics of ratio changes of Ca_i^{2+} under various physiological and pathological conditions in Tyrode-perfused beating hearts.

ACKNOWLEDGMENTS

We thank Albert Lind for help with the experiments.

GRANTS

This study was supported in part by a grant from the Netherlands Heart Foundation (grant no. 95.157). The developed software is available for use and can be obtained from O. Eerbeek.

REFERENCES

1. **Arkhammar PT, Nilsson T, and Bergren PO.** Glucose-stimulated efflux of Indo-1 from pancreatic beta-cells is reduced by probenecid. *FEBS Lett* 273: 182–184, 1990.
2. **Ashruf JF, Coremans JMCC, Bruining HA, and Ince C.** Increase of cardiac work is associated with decrease of mitochondrial NADH. *Am J Physiol Heart Circ Physiol* 269: H856–H862, 1995.
3. **Ashruf JF, Ince C, and Bruining HA.** Regional ischemia in hypertrophic Langendorff-perfused rat hearts. *Am J Physiol Heart Circ Physiol* 277: H1532–H1539, 1999.
4. **Auffermann W, Stefenelli T, Wu ST, Parmley WW, Wikman-Coffelt J, and Mason DT.** Influence of positive inotropic agents on intracellular calcium transients. Part I. Normal rat heart. *Am Heart J* 118: 1219–1227, 1989.
5. **Avontuur JAM, Bruining HA, and Ince C.** Inhibition of nitric oxide synthesis causes myocardial ischemia in endotoxemic rats. *Circ Res* 76: 418–425, 1995.
6. **Backx PH and Ter Keurs HEDJ.** Fluorescent properties of cardiac trabeculae microinjected with fura-2 salt. *Am J Physiol Heart Circ Physiol* 264: H1098–H1110, 1993.
7. **Baker AJ, Brandes R, Schreur JHM, Camacho SA, and Weiner MW.** Protein and acidosis after calcium-binding and fluorescence spectra of the calcium indicator indo-1. *Biophys J* 67: 1646–1654, 1994.
8. **Bátkai S, Rácz IB, Ivanics T, Toth A, Hamar J, Slaaf DW, Reneman RS, and Ligeti L.** An in vivo model to study the dynamics of intracellular free calcium changes in slow- and fast-twitch muscle fibers. *Pflügers Arch* 438: 665–670, 1999.
9. **Brandes R, Figueredo VM, Camacho SA, Massie BM, and Weiner WM.** Suppression of motion artifacts in fluorescence spectroscopy of perfused hearts. *Am J Physiol Heart Circ Physiol* 263: H972–H980, 1992.
10. **Brandes R, Figueredo VM, Camacho SA, Baker AJ, and Weiner MW.** Investigation of factors affecting fluorometric quantitation of cytosolic [Ca^{2+}] in perfused hearts. *Biophys J* 65: 1983–1993, 1993.
11. **Choi BR and Salama G.** Simultaneous maps of optical action potentials and calcium transients in guinea-pig hearts: mechanisms underlying concordant alternans. *J Physiol* 529: 171–188, 2000.

11a. **Del Nido PJ, Glynn P, Buenaventura P, Salama G, and Koretsky P.** Fluorescence measurements of calcium transients in perfused rabbit heart using Rhod 2. *Am J Physiol Heart Circ Physiol* 274: H728–H741, 1998.

12. **Duchen MR.** Contributions of mitochondria to animal physiology: from homeostatic sensor to calcium signalling and cell death. *J Physiol* 516: 1–17, 1999.
13. **Eerbeek O and Ince C.** Weak spots inside the myocardium of a Langendorff rat heart observed by NADH videofluorometry. *Adv Exp Med Biol* 411: 347–351, 1997.
14. **Figueredo VM, Brandes R, Weiner MW, Massie BM, and Camacho SA.** Endocardial versus epicardial differences of intracellular free calcium under normal and ischemic conditions in perfused rat hearts. *Circ Res* 72: 1082–1090, 1997.
15. **Fralix TA, Heineman FW, and Balaban RS.** Effects of tissue absorbance on NAD(P)H and Indo-1 fluorescence from perfused rabbit hearts. *FEBS Lett* 262: 287–292, 1990.
16. **Gray RA, Pertsov AM, and Jalife J.** Spatial and temporal organization during cardiac fibrillation. *Nature* 392: 75–78, 1998.
17. **Grynkiewicz G, Poenie M, and Tsien RY.** A new generation of Ca^{2+} indicators with greatly improved fluorescent properties. *J Biol Chem* 260: 3440–3350, 1985.
18. **Gwathmey JK and Morgan JP.** Altered calcium handling in experimental pressure-overload hypertrophy in the ferret. *Circ Res* 57: 836–843, 1985.
19. **Ince C, Ashruf JF, Avontuur JA, Wieringa PA, Spaan JAE, and Bruining HA.** Heterogeneity of the hypoxic state in the rat heart is determined at capillary level. *Am J Physiol Heart Circ Physiol* 264: H294–H301, 1993.
20. **Kloner RA, Boili R, Maarbau E, Reinlib L, and Braunwald E.** Medical and cellular implications of stunning, hibernation and preconditioning. An NHLBI workshop. *Circulation* 97: 11848–1867, 1998.
21. **Laurita KR and Singal A.** Mapping action potentials and calcium transients simultaneously from the intact heart. *Am J Physiol Heart Circ Physiol* 280: H2053–H2060, 2001.
22. **Lee HC, Mohabir R, Smith N, Franz R, and Clusin WT.** Effect of ischaemia on calcium-dependent fluorescence transients in rabbit hearts containing Indo-1. *Circulation* 78: 1047–1059, 1988.
23. **Li T, Sperelakis N, Teneick RE, and Solaro RJ.** Effects of diacetyl monoxime on cardiac excitation-contraction coupling. *J Pharmacol Exp Ther* 232: 688–695, 1985.
24. **Lorell BH, Apstein CS, Cunningham MJ, Schoen FJ, Weinberg EO, Peeters GA, and Barry WH.** Contribution of endothelial cells to calcium-dependent fluorescence transients in rabbit hearts loaded with Indo-1. *Circ Res* 67: 313–328, 1990.
25. **Marban E and Koretsune Y.** Cell calcium, oncogenesis and hypertrophy. *Hypertension* 15: 652–658, 1990.
26. **Meisner A and Morgan JP.** Contractile dysfunction and abnormal Ca^{2+} modulation during postischemic reperfusion in rat heart. *Am J Physiol Heart Circ Physiol* 268: H100–H111, 1995.

27. **Minamikawa T, Cody SH, and Williams DA.** In situ visualization of spontaneous calcium waves within perfused whole rat heart by confocal imaging. *Am J Physiol Heart Circ Physiol* 272: H236–H243, 1997.
28. **Mittmann C, Eschenhagen E, and Scholz H.** Cellular and molecular aspects of contractile dysfunction in heart failure. *Cardiovasc Res* 39: 267–275, 1998.
29. **Morgan JP.** Abnormal intracellular modulation of calcium as major cause of cardiac contractile dysfunction. *N Engl J Med* 325: 625–632, 1991.
31. **Pertsov AM, Davidenko JM, Salomonsz R, Baxter WT, and Jalife J.** Spiral waves of excitation underlie reentrant activity in isolated cardiac muscle. *Circ Res* 72: 631–650, 1993.
32. **Reuter H.** Electrophysiology of calcium channels in the heart. In: *Calcium Antagonists and Cardiovascular Disease*, edited by Opie LH. New York: Raven, 1984, p. 43–51.
33. **Salama G, Lombardi R, and Elson J.** Maps of optical action potentials and NADH fluorescence in intact working hearts. *Am J Physiol Heart Circ Physiol* 252: H384–H394, 1987.
34. **Scaduto RC Jr and Grotyohann LW.** 2,3-Butanedione monoxime unmasks Ca^{2+}-induced NADH formation and inhibits electron transport in rat hearts. *Am J Physiol Heart Circ Physiol* 279: H1839–H1848, 2000.
35. **Scaduto RC Jr and Grotyohann LW.** Hydrolysis of Ca^{2+}-sensitive fluorescent probes by perfused rat heart. *Am J Physiol Heart Circ Physiol* 285: H2118–H2124, 2003.
36. **Spurgeon HA, Stern MD, Baartz G, Raffeli S, Hansford R, Talo A, Lakatta EG, and Capogrossi MC.** Simultaneous measurements of Ca^{+}, concentration and potential in cardiac myocytes. *Am J Physiol Heart Circ Physiol* 258: H574–H586, 1990.
37. **Stefenelli T, Wikman-Coffelt J, Wu ST, and Parmley WW.** Calcium-dependent fluorescence transients during ventricular fibrillation. *Am Heart J* 120: 590–597, 1990.
38. **Wiltkink A, Nijweide PJ, Scheenen WJJM, Ypey DL, and van Duijn B.** Cell membrane stretch in osteoclasts triggers a self-reinforcing Ca^{2+}-entry pathway. *Pflügers Arch* 429: 663–671, 1995.
39. **Wikman-Coffelt J, Wu ST, and Parmley WW.** Intracellular endocardial calcium and myocardial function in rat hearts. *Cell Calcium* 12: 39–50, 1991.
40. **Witkowski FX, Leon LJ, Penkoske PA, Giles WR, Spanoll ML, Ditto WL, and Winfree AT.** Spatiotemporal evolution of ventricular fibrillation. *Nature* 392: 78–82, 1998.